Water Research 252 (2024) 121189

Contents lists available at ScienceDirect

Water Research

journal homepage: www.elsevier.com/locate/watres

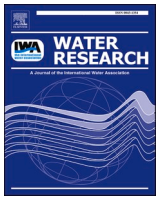

Synergistic effect of UV-A and UV-C light is traced to UV-induced damage of the transfer RNA

Sandra Probst-Rüd [a,b], Paul Onkundi Nyangaresi [c], Adefolawe A. Adeyeye [c], Martin Ackermann [a,b], Sara E. Beck [b,c,*], Kristopher McNeill [a,*]

[a] Department of Environmental Systems Science, Institute of Biogeochemistry and Pollutant Dynamics (IBP), ETH Zurich, Zurich, Switzerland
[b] Department of Environmental Microbiology, Eawag: Swiss Federal Institute of Aquatic Science and Technology (Eawag), Dubendorf, Switzerland
[c] Department of Civil Engineering, University of British Columbia, Vancouver, Canada

ARTICLE INFO

Keywords:
UV inactivation mechanisms
tRNA
Synergistic effect
Combined wavelengths
UV LEDs
E. coli

ABSTRACT

UV light emitting diodes (LEDs) are considered the new frontier of UV water disinfection. As UV technologies continue to evolve, so does the need to understand disinfection mechanisms to ensure that UV treatment continues to adequately protect public health. In this research, two *Escherichia coli (E. coli)* strains (the wild type K12 MG1655 and K12 SP11 (ThiI E342K)) were irradiated with UV-C at 268 nm both independently and after exposure to UV-A (365 nm). A synergistic effect was found on the viability of the wild type *E. coli* K12 strain when UV-A irradiation was applied prior to UV-C. Sublethal UV-A doses, which had a negligible effect on cell viability alone, enhanced UV-C inactivation by several orders of magnitude. This indicated a specific cellular response mechanism to UV-A irradiation, which was traced to direct photolysis of the transfer RNA (tRNA), which are critical links in the translation of messenger RNA to proteins. The wild type K12 strain MG1655, containing tRNAs with a thiolated uridine, directly absorbs the UV-A light, which leads to a reduction in protein synthesis, making them more susceptible to UV-C induced damage. However, the K12 strain SP11 (ThiI E342K), with a point mutation in the *thiI* gene that prevents a post-transcriptional modification of tRNA, experienced less inactivation upon subsequent irradiation by UV-C. The growth rate of cells, which was inhibited by sublethal UV-A doses, was not inhibited in this mutant strain with the modified tRNA. Time-lapse microscopy with microfluidics showed that sub-lethal UV-A caused a transient, reversible, growth arrest in *E. coli*. However, once the growth resumed, the cell division time resembled that of unirradiated cells. Damage induced by UV-A impaired the recovery of damage induced by UV-C. Depending on the UV-A dose applied, the synergistic effect remained even when there was a time delay of several hours between UV-A and UV-C exposures. The effect of sublethal UV-A was reversible over time; therefore, the synergistic effect was strongest when UV-C was applied immediately after UV-A. Combining UV-A and UV-C irradiation may serve as a practical tool to increase UV disinfection efficacy, which could potentially reduce costs while still adequately protecting public health.

1. Introduction

Bacterial contamination of drinking water is a significant global public health concern. At least 2 billion people worldwide rely on a drinking water source that is contaminated with microorganisms, posing the highest risk to the safety of drinking water (WHO, 2022). Therefore, effective water disinfection is of utmost importance. Disinfection is commonly achieved through chlorination, ultraviolet (UV) light, chloramines, or ozone treatment (Ishaq et al., 2018). Disinfection by UV light has several advantages: it does not require the addition of chemicals nor change the taste, has a lower risk of producing disinfection by-products, and there is no known risk of applying excessive doses, which are challenges associated with chemical disinfectants. Effectiveness of UV disinfection varies depending on the wavelength and the specific microorganism being targeted (Itani and El Fadel, 2023; Martin-Somer et al., 2023). UV light is typically categorized into four wavelength ranges: vacuum UV (100–200 nm), UV-C (200–280 nm), UV-B (280–315 nm), and UV-A (315–400 nm) (Meulemans, 1987). The

* Corresponding author at: Department of Civil Engineering, University of British Columbia, Vancouver, Canada and Department of Environmental Systems Science, Institute of Biogeochemistry and Pollutant Dynamics (IBP), ETH Zurich, Zurich, Switzerland.
E-mail addresses: sara.beck@ubc.ca (S.E. Beck), kris.mcneill@env.ethz.ch (K. McNeill).

https://doi.org/10.1016/j.watres.2024.121189
Received 16 October 2023; Received in revised form 22 January 2024; Accepted 23 January 2024
Available online 24 January 2024

UV-C range, commonly referred to as germicidal UV, acts through direct photolysis, by inducing damage to DNA and other biomolecules, resulting in a germicidal effect (Beck et al., 2018; Besaratinia et al., 2011; Cadet et al., 2005). However, a significant challenge with UV-C disinfection is that the UV-C doses applied need to exceed the doses required for total inactivation (no colonies observed after inactivation) in order to prevent the repair of damaged bacterial cells or the growth of surviving bacteria, which can lead to the resurgence of potentially pathogenic bacteria (Nyangaresi et al., 2023). This can be a drawback if the water is not consumed immediately.

Although light in the UV-A range lies outside of the DNA absorption spectra, such light at a UV-A dose of approximately 52,000 mJ/cm^2 also has a proven germicidal effect from indirect photolysis, attributed to increased levels of reactive oxygen species, which in turn damage the cellular or viral structure, or DNA and RNA (Hamamoto et al., 2007; Jiang et al., 2009; Song et al., 2019). At lower doses, UV-A can have sublethal effects on *E. coli,* causing oxidative stress, a reduction in protein synthesis, and a delay in growth (Hoerter et al., 2005). It has been shown that some of these sublethal effects are based on the direct absorption of the UV-A light by the tRNAs, namely the 4-thiouridine (s^{4}U) within the tRNA (Probst-Rüd et al., 2017) as shown in the Supplementary Information (Fig. S1). Unlike standard DNA and RNA nucleotides, which absorb in the UV-C range, s^{4}U has a broad absorption range with a maximum at ~330 nm, which is within the UV-A range (Bommisetti and Bandarian, 2022). The post-transcriptional incorporation of s^{4}U into tRNAs is facilitated by the protein ThiI, a sulfur transferase involved in the biosynthetic pathway of thiamine and s^{4}U in tRNAs (Bosshard, 2010; Čavužić and Liu, 2017). It has been shown that strains lacking ThiI show a reduced growth delay, a higher induction of the SOS response and a higher survival upon UV-A irradiation compared to strains with a functional copy of *thiI* (Caldeira de Araujo and Favre, 1986; Favre et al., 1986; Thiam and Favre, 1984). Upon UV-A irradiation of tRNAs, the thiouridine crosslinks to a cysteine (Thomas and Favre, 1975). Crosslinked tRNAs lead to a reduction in protein synthesis; therefore, tRNA absorption of UV-A leads to a reduced protein synthesis (Ramabhadran and Jagger, 1976).

Previous studies have demonstrated that UV-A exposure impairs the repair of thymine dimers, and UV-A light can interact with ionizing radiation from UV-C to deactivate microorganisms (Martin-Somer et al., 2023). Furthermore, sublethal UV-A light exhibits a synergistic effect with UV-B light in a ThiI-dependent manner (Probst-Rüd et al., 2017). It is worth noting that delivering sublethal doses of UV-A are more practical than administering lethal doses, making it suitable for real-world applications. While UV-A light is significantly less bactericidal compared to UV-C light, the sublethal effects of UV-A may be more relevant for potential synergies than its germicidal action (Martin-Somer et al., 2023). Additionally, sublethal UV-A light is advantageous for technical applications due to its limited dosage, resulting in shorter disinfection times. Furthermore, the inclusion of UV-A light may prolong the effects of UV-C disinfection by impeding DNA damage repair and protein synthesis, which would also limit the growth of surviving cells (Song et al., 2019a). Consequently, the emergence of ultraviolet light-emitting diodes (UV LEDs), which offer a range of wavelengths, provides an opportunity to combine UV-C and UV-A wavelengths in compact devices suitable for point-of-use applications. By integrating these two wavelengths in disinfection systems, overall costs could potentially be reduced as fewer UV-C LEDs would be required in the design, considering that UV-A LEDs are more efficient and currently easier and cheaper to manufacture than the UV-C LEDs (Kneissl et al., 2019). Therefore, in this study, we investigated the effect of sublethal UV-A LED exposure on *E. coli* cell growth and on UV-C LED inactivation of *E. coli* at the molecular level.

2. Experimental procedures

To determine the sublethal UV-A doses, we measured the inactivation at different UV-A doses and evaluated the survival rate. To investigate the interaction between UV-A and UV-C light exposure in the inactivation of *E. coli*, we examined the impact of UV-C light on *E. coli*, both with and without pre-exposure to UV-A light. Specifically, we subjected *E. coli* K12 MG1655 cultures to UV-A light (at 365 nm) followed by UV-C light (at 268 nm) at various doses.

To assess the effect of UV-A pre-exposure on UV-C inactivation, we investigated cell growth and UV inactivation of the wild-type *E. coli* strain in comparison with a mutated strain of *E. coli* that lacks s^{4}U-modified tRNAs, which are responsible for UV-A absorption. Specifically, we measured the growth of both strains and also exposed the wild-type and *thiI* mutant *E. coli* strains separately to predetermined sublethal doses of UV-A irradiation, followed by 20 mJ/cm^2 UV-C irradiation.

To observe the behavior of individual cells upon UV-A irradiation, we conducted single-cell observations by time-lapse microscopy in a microfluidics device. The effect of the time delay between UV-A and UV-C exposure was investigated to determine the effect of time on the cells' ability to recover from UV-A exposure prior to UV-C. Finally, we investigated the effect of sample measurement time, to determine whether sample measurements at 0 or 24 h affected the photoinactivation or recovery.

2.1. Bacterial strains

The *E. coli* strains used in this study were the wild type K12 strain MG1655, and the K12 strain SP11 (ThiI E342K), a strain with a point mutation in *thiI* (Probst-Rüd et al., 2017). As described in Probst-Rüd et al. (2017), SP11 was derived from the wild-type strain through selection for resistance to simultaneous exposure to UV-A and UV-B; its only difference to MG1655 was a point mutation in the gene *thiI*, which prevents the post-transcriptional modification s^{4}U8 in tRNAs.

2.2. Cultivation

In each experiment, four cultures were propagated by adding a single bacterial colony to 4 mL sterile Luria-Bertani broth (Sigma-Aldrich) and incubated in a shaking incubator (37 °C, 220 rpm) overnight. For batch cultivation, 4 mL of M9 minimal medium, containing M9 minimal salts (Sigma-Aldrich), 10 mM glucose, 1 mM $MgSO_4$, and 0.1 mM $CaCl_2$, were inoculated with 40 μL of the overnight culture and incubated in a shaking incubator (37 °C, 220 rpm) for approximately five hours until OD_{600} of 0.6–0.7 was reached. Cells from the batch culture were harvested by centrifugation (4000 g, 10 min) and washed with sterile M9 buffer (1 x M9 minimal salts, Sigma-Aldrich). The cells were then diluted with M9 buffer to an OD_{600} of 0.1.

2.3. UV light sources and dose determination

The UV-A light source used was a UV-A LED LC-L1V3 (Hamamatsu) emitting at 365 nm with a full width at half maximum (FWHM) of 10 nm and a maximum irradiance of 14,000 mW/cm^2. The lamp was operated at 80 % of the maximum intensity while equipped with a collimated head (Hamamatsu Photonics, L11922–01). The light intensity on the sample was determined using a two-component chemical actinometer solution of p-nitroanisole (PNA) and pyridine (pyr), which are known to have the advantage of adjustable quantum yields. The light intensity reaching the sample was measured across various light intensities and experiment durations (Dulin and Mill, 1982; Laszakovits et al., 2017). PNA concentrations were determined by HPLC (Dionex, UltiMate 3000 LC) with an Ascentis RP-Amide C18, 4.6 × 250 mm, a 5 μm particle size column, with a mobile phase composition of 65:35 ACN:H2O and a flow rate of 1 mL/min. The absorbance was monitored with a photodiode array detector at 314 nm. Actinometry was performed before and after the majority of the experiments and showed consistently-stable irradiance. The average irradiance measured throughout the water sample

was 1.99 mW/cm^2. For details of the actinometry method, including the absorbance spectrum of PNA, we refer the reader to Laszakovits et al. (2017). Time-lapse microscopy experiments used a different UV-A light source as described below.

The UV-C light source used was a UV-C LED Pearl Beam (AquiSense) equipped with 3 × 265 nm UV-C LEDs emitting at a peak wavelength of 268 nm with a FWHM of 14 nm. Average UV doses applied to a water sample 3 cm from the light source were determined through radiometry as described previously (Beck et al., 2017; Nyangaresi et al., 2023), adjusting for reflection off the water surface (reflection factor: 0.975), UV absorbance (measured by a Thermo Fisher Scientific UV–Vis spectrophotometer), depth of the water sample (0.2 cm), and the non-uniform distribution of light across the sample surface (Petri factor: 0.982). The incident irradiance was measured with an ILT2400 radiometer with SED270 detector (International Light, USA). Average irradiance throughout the water sample was calculated at 0.489 mW/cm^2. For dose calculations, the average UV dose was determined from the product of average irradiance and the UV irradiation time.

2.4. UV light exposure

For UV-inactivation and synergy experiments, samples were prepared as described above including dark controls, which were handled the same way as the irradiated samples. Aliquots of 6 mL were exposed to UV-A light in 15 mL borosilicate test tubes. For irradiation, the lamp was fixed to the open top of a test tube containing the sample (Fig. S2 in the Supplementary Information). The distance from the lamp head to the water samples was 2 cm. Unless stated otherwise, the samples were irradiated with UV-C directly following the UV-A exposure. For UV-C irradiation, 1 mL of the samples was transferred to a Petri dish (60 mm x 15 mm) containing 4 mL of M9 buffer. The UV-C lamp was placed on top of the open Petri dish (Fig. S2). During irradiation, the samples were stirred with a magnetic stirrer. To maintain sterility, the irradiation was performed on a sterile bench. No increase in sample temperature was detected during the experiments.

2.5. Plate count assay

Bacterial inactivation was quantified using a colony-forming assay. Unless otherwise stated, the irradiated samples and the dark controls were sampled before and after UV-A irradiation of 0 min, 5 min or 10 min (0, 600 and 1200 mJ/cm^2). During UV-C irradiation, the samples were sampled every 5 s for up to 30 s (0, 2.5, 5, 7.5, 10, 12.5 and 15 mJ/cm^2). The bacterial suspensions were serially diluted in M9 buffer; appropriate dilutions were plated on M9 agar plates (M9 media with 1.5 % agar (Sigma-Aldrich)) and incubated at 37 °C for 48 h. The colonies were counted following the incubation. The survival was calculated using the following equation:

$$survival = \left(\frac{cfu_t}{cfu_0}\right)$$

where cfu_0 is the original colony count (colony forming units) at time = 0 and cfu_t is the colony count at time t.

2.6. Cell growth curves

To measure cell growth after exposure to UV-A light of different doses, the samples were irradiated in M9 buffer, diluted into M9 minimal medium in 96-well plates and the optical density was measured by a microplate absorbance spectrophotometer (Biotek). The experiment was conducted with three independent cultures and the two different strains described above.

2.7. Quantitative time-lapse microscopy

The microfluidic devices used for time-lapse microscopy in these experiments were similar to those described by Wang et al. (2010) and adapted by Arnoldini et al. (2014). The setup consisted of a glass slide with a Polydimethylsiloxane elastomer (PDMS) structure attached. Each PDMS chip contained eight separate flow channels, which included narrow side channels (0.9 × 20 μm) where the cells grew. Each flow channel was loaded with 5 μL of a different batch culture. As the cells grew, they were displaced from these narrow channels into the wider flow channel, which supplied nutrients (M9 media, as previously described), and were subsequently removed by the medium flow. The media was pumped through the device at a rate of 0.4 mL/h using syringe pumps (New Era). Cell imaging was conducted using an inverted Olympus X81 microscope with ZDC focus hardware, equipped with an oil objective (Olympus UPLFLN100x), an automated stage (Marzhauser Scan IM 120×80), and an incubation chamber (Life Imaging Services), enabling precise temperature control at 37 °C. For the light conditions, UV-A irradiation was applied through the 100x objective using a 120 W mercury short arc lamp (X-cite 120 PC Q) with a bandpass filter (ET365/10x, Chroma; Dichroic mirror: U-MWU2: BP 330–385 / DM 400 / LP 420). The intensity of the light throughout the sample (20 mW/cm^2) was measured using a microscope slide photodiode power sensor (Thorlabs, PM100D). Meanwhile, image recording and analysis used a cooled CCD camera (Olympus XM10). The Xcellence Pro-software package (Olympus, Version 1.2) was employed for image acquisition, and subsequent analysis was performed using ImageJ. A previously-described plugin (CellCounter, developed by Kurt de Vos, University of Sheffield) was adapted for image analysis (Mathis and Ackermann, 2016).

2.8. Statistical analysis

The difference between samples that were exposed to sublethal UV-A before UV-C and those that were not were determined using analysis of variance (ANOVA). For statistical analysis of the cell growth experiments, the lag times were estimated as time until the optical density (at 600 nm) reached 0.1. In addition, the effect of pre-exposure of UVA on the two strains were analyzed by carrying out regression. ANOVA was used to test the significance of dark controls and comparison between viable cells immediately and twenty-four hours after. All data visualization and statistical analysis were carried out in R Studio (Version 2022.07.2 + 576 "Spotted Wakerobin" Release).

3. Results and discussion

3.1. Interaction of UV-A and UV-C light exposure during inactivation of *E. coli*

At 0, 600 and 1200 mJ/cm^2 of UV-A irradiation, a negligible decrease in survival could be detected (Fig. 1). Meanwhile, after 1800, 2400 and 3600 mJ/cm^2 of UV-A exposure, the number of cells decreased exponentially with a decrease of 0.65, 1.1 and 2.0 $\log_{10}$ units, respectively (Fig. 1). After more than 3600 mJ/cm^2 of UV-A exposure, no surviving cells could be detected with the plate count assay. Therefore, for subsequent experiments, we applied 600 and 1200 mJ/cm^2 doses of UV-A, which negligibly reduced the survival of the *E. coli* K12 MG1655.

UV-C inactivation was measured by exposing the samples to 2.5, 5.0, 7.5 and 10 mJ/cm^2. The inactivation curve of UV-C light alone showed a small shoulder followed by an exponential decay (Fig. 2), which has also been reported in the literature (Nyangaresi et al., 2018). After 10 mJ/cm^2 of UV-C exposure, 99.75 ± 0.07 % (mean ± SE) of the cells were inactivated, which corresponded to a decrease of 2.6 $\log_{10}$ units (Fig. 2). A significant increase in inactivation was observed when the samples were pre-exposed to sublethal UV-A, demonstrating a statistically significant difference compared to the cells not pre-exposed to

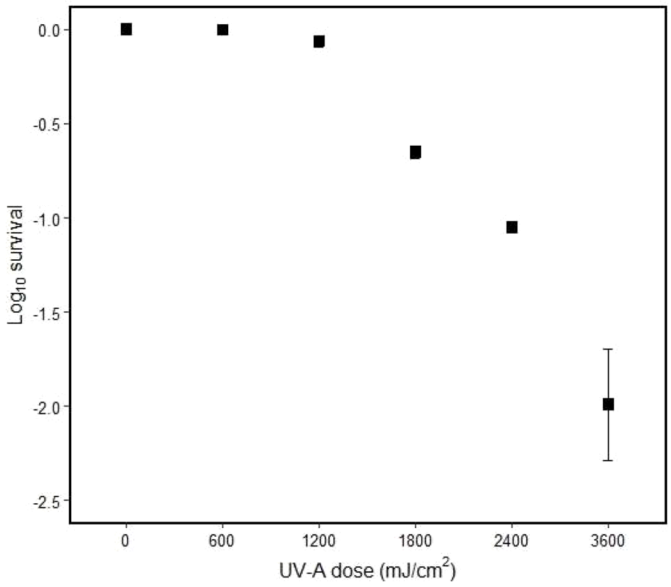

Fig. 1. Inactivation of the wild type *E. coli* K12 by UV-A light exposure. An exponential decrease of viable cells was seen after irradiating with a UV-A dose of 1200 mJ/cm^2. Each point represents the log of the ratio between the number of colony forming units per mL (cfu/mL) obtained at a certain UV dose relative to the cfu/mL at time zero. Error bars represent the standard error from duplicate independent experiments.

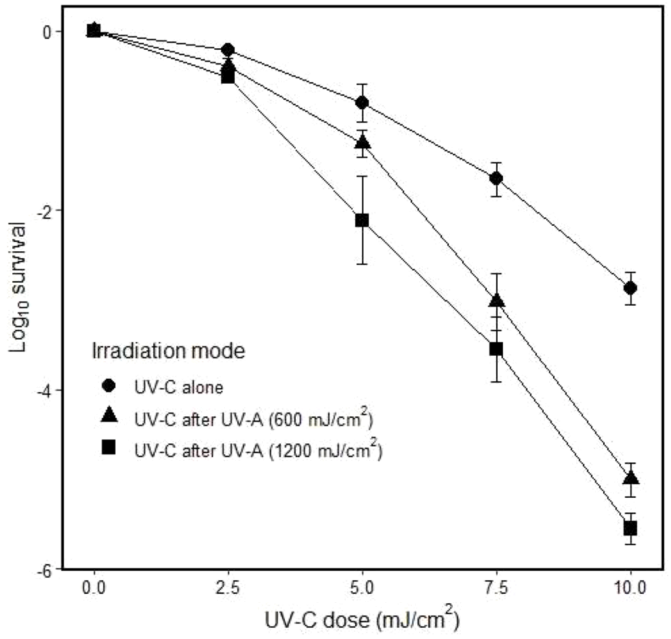

Fig. 2. Number of viable wild type *E. coli* K12 cells for different combinations of UV-C and UV-A irradiations. The decrease in viable cells was greater in cells irradiated with both UV-A and UV-C, with the cells with a higher dose of UV-A experiencing the greatest decline. Error bars represent the standard error of five independent experimental replicates.

UV-A (p = 4.6E-09) (Fig. 2). Pre-exposing the cells to 600 and 1200 mJ/cm^2 of UV-A, followed by 10 mJ/cm^2 of UV-C irradiation, resulted in a decrease of 5.1 and 5.7 $\log_{10}$ units. This represented an additional reduction of 2.5 to 3.1 $\log_{10}$ units compared to UV-C alone. The findings confirm that despite the UV-A dose having only a small effect on cell viability, UV-A and UV-C act synergistically in inactivating *E. coli*.

To understand the nature of the synergistic effect, it is important to initially consider the individual effects of UV-A and UV-C irradiation on the cell. UV-C damage primarily occurs through direct photolysis, i.e. direct light absorption by DNA, leading to DNA damage (Song et al., 2019a). This is attributed to the fact that the DNA has a relative UV absorption peak at 260 nm (Beck et al., 2015), which is close to the peak UV-C LED wavelength (268 nm) applied in this work. In contrast, UV-A irradiation acts through direct and indirect photolysis; at sublethal levels, it can induce oxidative stress, growth delay and reduced protein production, possibly due to UV-A absorption by tRNAs (Hoerter et al., 2005). Our experimental findings revealed that the lag-phase can be significantly prolonged by several hours for irradiated samples of the wild type K12 strain MG1655, depending on the intensity of the applied UV-A light in comparison to unirradiated cells (Fig. 3a and c). However, the additional time lag observed for growth of irradiated samples almost disappears when using the K12 strain SP11 (ThiI E342K), a strain with a non-functional *thiI* gene (Fig. 3b and c). Furthermore, the extended lag-phase, which is absent in this mutant with the non-functional *thiI* gene, is not caused by cell death, as survival remained relatively constant during exposure to sublethal doses of UV-A (Fig. 3a and b insets). These findings align with previous reports, suggesting that UV-A light absorption by tRNAs with post-transcriptional s^{4}U modifications triggers a direct photoreaction that reduces the amino acid charging capacity, leading to an accumulation of uncharged tRNAs, subsequent growth arrest and reduced protein production via the stringent response (Ćavužić and Liu, 2017; Bommisetti and Bandarian, 2022; Sun et al., 2020; Dai et al., 2023). Therefore, the growth delay induced by UV-A light appears to be dependent upon the presence of s^{4}U modifications in tRNAs, as inferred from the literature and demonstrated in this study (Fig. S1).

However, the aforementioned finding does not provide insights into the responses at the single-cell level that contribute to the extended lag phase. For example, do all cells stop growing, or do they simply grow at a slower rate? How variable is the time it takes for growth to resume? We addressed these questions using quantitative time-lapse microscopy across 12 representative cell lineages (Fig. 4a). The results revealed that after one minute (1200 mJ/cm^2) of UV-A irradiation, all cells temporarily ceased growth and the duration to resume growth depended on the UV dose (Fig. 4b). Notably, even with 30 s (600 mJ/cm^2) of UV-A irradiation, the time until the first division after irradiation significantly (p = 2.7E-06) differed from that of unirradiated cells. Interestingly, once the growth resumed, the division time resembled that of unirradiated cells (Fig. 4b). These experiments demonstrate that the observed growth delay in cell cultures stems from a transient growth arrest affecting most or all of the cells exposed to UV-A light. Therefore, it is plausible that the absorbance of UV-A light by tRNAs plays a crucial role in the synergistic effect of UV-A and UV-C light.

3.2. ThiI: the critical enzyme for the interaction of UV-A and UV-C irradiation

In Section 3.1, we determined the sublethal doses of UV-A on *E. coli* at 600, and 1200 mJ/cm^2. To assess the effect of sublethal UV-A pre-exposure on UV-C inactivation for both cell types, we subjected both the wild type and ThiI mutant *E. coli* strains to separate exposures of 0 and 600 mJ/cm^2 of UV-A irradiation, followed by 20 mJ/cm^2 UV-C irradiation (Fig. 5). Although the effect of UV-C alone was comparable for both strains, pre-exposure to 600 mJ/cm^2 of UV-A irradiation significantly affected the wild type strain (Multiple Linear Regression, Strain, UV-A X UV-C, p = 2.3E-05), as shown in Fig. 5. However, the effect of UV-A pre-exposure on the UV-C inactivation of the ThiI mutant was not statistically significant (Multiple Linear Regression, Strain, UV-A X UV-C, p = 0.29). These results indicate that the synergistic effect of UV-A and UV-C light depends on the presence of the s^{4}U-modification in tRNAs.

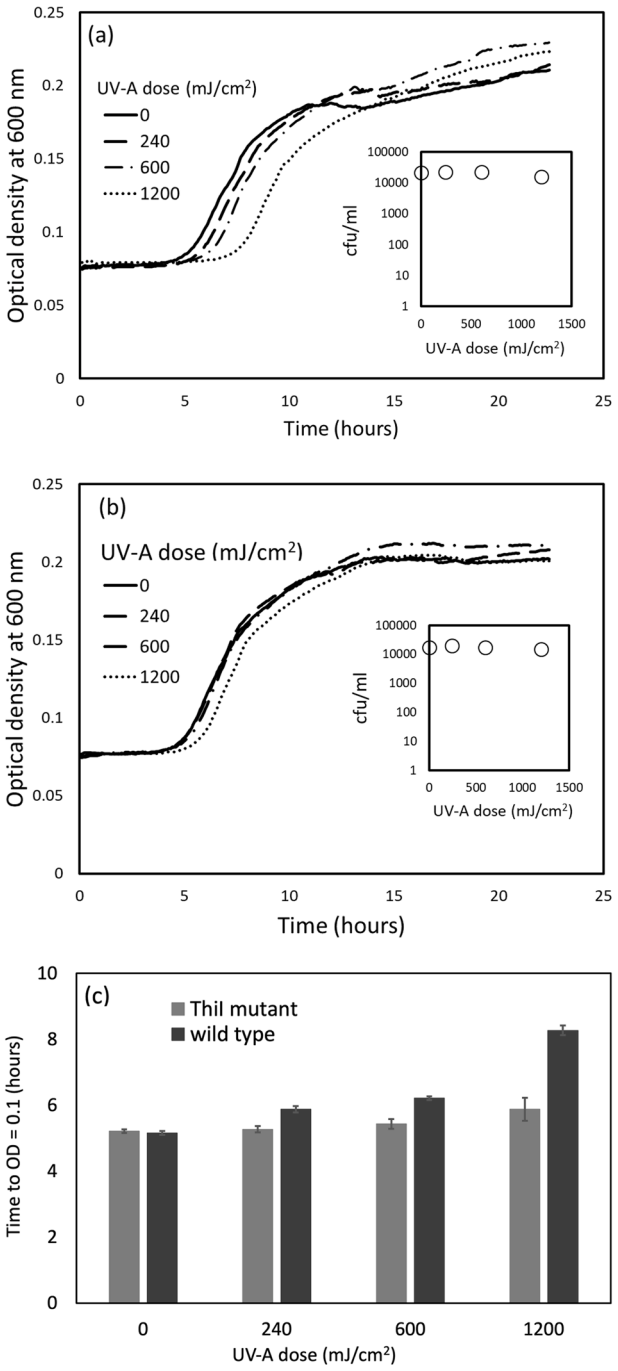

Fig. 3. Growth of (a) wild type K12 strain MG1655 (b) the K12 strain SP11 (ThiI E342K), a ThiI mutant, *E. coli* strains after exposure to UV-A light of different doses and (c) represents the time it took both strains to reach an optical density (OD) of 0.1, with error bars representing standard error ($n = 3$). In the ThiI mutant strain, in which tRNAs do not include s^4U and therefore do not absorb UV-A, the growth rate was less inhibited by UV-A exposure.

3.3. UV dose and time-dependence of the synergistic effect

The next objective was to investigate the dependence of the synergistic interaction between UV-A and UV-C irradiation on the dose and the timing of the two irradiations in wild type *E. coli*. The aforementioned findings showed that the synergistic interaction between UV-A and UV-C was mostly unaffected by the dose of UV-A irradiation (Fig. 2). This observation contradicts the interaction between UV-A and UV-B light, which relies on the intensities of both light sources (Probst-Rüd et al., 2017). One possible explanation for this apparent difference is that, in the case of the UV-A and UV-C interaction, a certain threshold of UV-A irradiation might be necessary to trigger cellular state changes that render bacterial cells sensitive to UV-C. The absence of interaction between UV-A and UV-C irradiation in the bacterial strain lacking UV-A absorbing tRNAs suggests that UV-A absorption by tRNAs induces this altered state. Notably, previous studies have demonstrated that the duration of effects resulting from UV-A absorption by tRNAs, such as growth delay and the shutdown of protein synthesis, is dose dependent (Jagger, 1983; Thiam and Favre, 1984). As illustrated in Fig. 3, the *E. coli* strain containing the UV-absorbing tRNAs exhibited delayed cellular growth that was dependent on the UV-A exposure. Therefore, even though the UV-A dose did not directly affect the synergy detected from applying UV-A prior to UV-C irradiation, the sensitivity of *E. coli* to UV-C light could have been influenced by the initial UV-A exposure depending on whether or not there was a time lag between the UV-A and the UV-C exposure.

To investigate the effect of the duration of UV-A irradiation on wild type *E. coli*, we varied the time interval between UV-A and UV-C irradiation. The samples were exposed to 0, 600 and 1200 mJ/cm^2 of UV-A irradiation, followed by a delay of 0, 8, 16 and 24 h before being irradiated with 10 mJ/cm^2 of UV-C. During the delay period, the cells were incubated in a buffer at 37 °C in the dark, to be in the optimal temperature range for *E. coli* and prevent photorepair. The effect of UV-A irradiation decreased as the delay time increased for both tested UV-A doses, although the inactivation effect remained more stable for the higher dose (Fig. 6). After 16 and 24 h of delay, the samples irradiated with 600 mJ/cm^2 of UV-A light prior to 10 mJ/cm^2 of UV-C were not significantly different from the dark controls ($p = 0.9$), indicating that the irradiated cells recovered from the UV-A exposure. Doubling the UV-A pre-exposure to 1200 mJ/cm^2 extended the recovery time, requiring 24-h delay before the synergistic effect disappeared (Fig. 6). These results suggest that the recovery from the UV-A induced state is prolonged when higher UV-A doses are applied. Consequently, the synergistic interaction between UV-A and UV-C irradiation is dose-dependent, particularly when there is a time delay between the irradiation with these two wavelengths.

3.4. Recovery is reduced by UV-A light

When applying UV disinfection for the treatment of drinking water, an important concern is the stability of the treated water, which refers to the duration before the number of viable bacteria begins to increase again due to growth or repair. Treated water remains stable only for a limited time, as damaged cells may undergo repair or a small fraction of survivors can regrow, even in nutrient-poor water (Bohrerova et al., 2015; Kollu and Örmeci, 2015). It is plausible that this recovery process can be minimized or delayed in water pre-treated with UV-A irradiation, as UV-A light has the potential to inhibit protein production and growth for a certain period, in a dose-dependent manner. Our subsequent objective was to investigate this hypothesis. To assess the effect of UV-A pre-exposure on the recovery of cells inactivated with UV-C light, we conducted a study to measure the colony-forming ability of cells at two different points: immediately after UV-C exposure and 24 h post-exposure. Specifically, we pre-exposed the samples to 600 mJ/cm^2 of UV-A irradiation or kept them in the dark. Subsequently, a time kill curve was measured with UV-C irradiation, with samples collected after every 5 s. A portion of these samples was diluted and plated immediately after the irradiation, while the remaining were incubated in the dark at 37 °C. After 24 h, the number of cells that were able to form a colony in each sample was determined. Interestingly, in samples exposed to UV-C irradiation, the count of cells capable of forming colonies was significantly higher after 24 h compared to the cell counts immediately following UV-C exposure (Fig. 7). Specifically, after applying 7.5 mJ/cm^2 of UV-C irradiation, there were approximately 10 times (1-log) more cultivable cells after 24 h in the dark compared to immediately

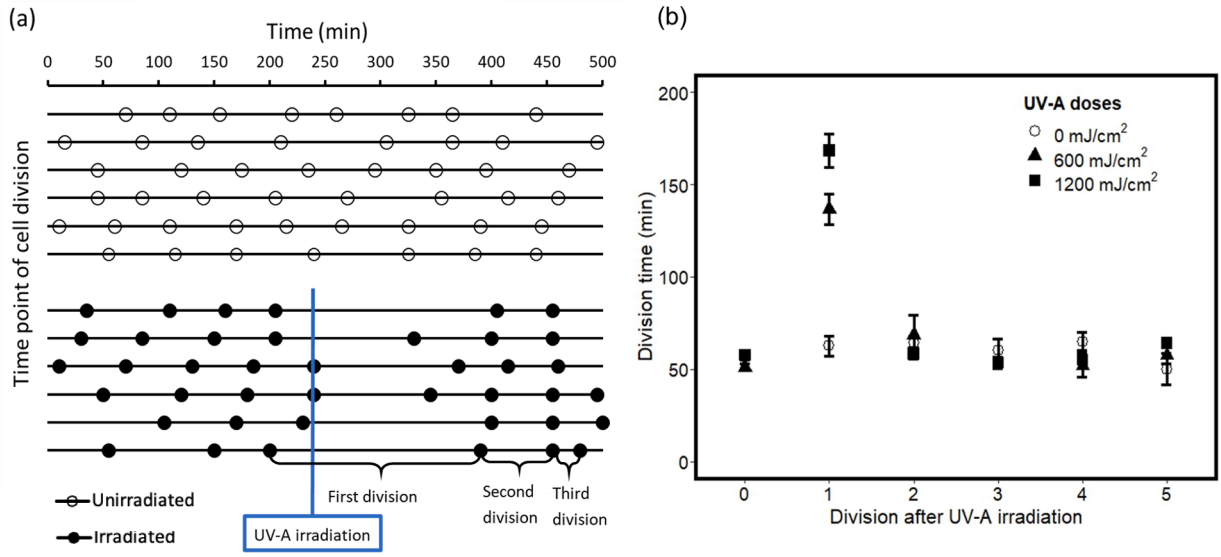

Fig. 4. Single cell measurements by time-lapse microscopy in a microfluidic device observed for 500 min: **(a)** representative data of 12 individual cells (6 not exposed to UV-A, and 6 exposed to 1200 mJ/cm^2 (60 s) of UV-A light) at minute 240. Each horizontal line represents one cell; the circles show the time point of cell divisions. **(b)** The interdivision interval (from one division to the next) with or without 600 or 1200 mJ/cm^2 (30 or 60 s) of exposure to UV-A. Error bars represent standard error of 3 independent experimental replicates.

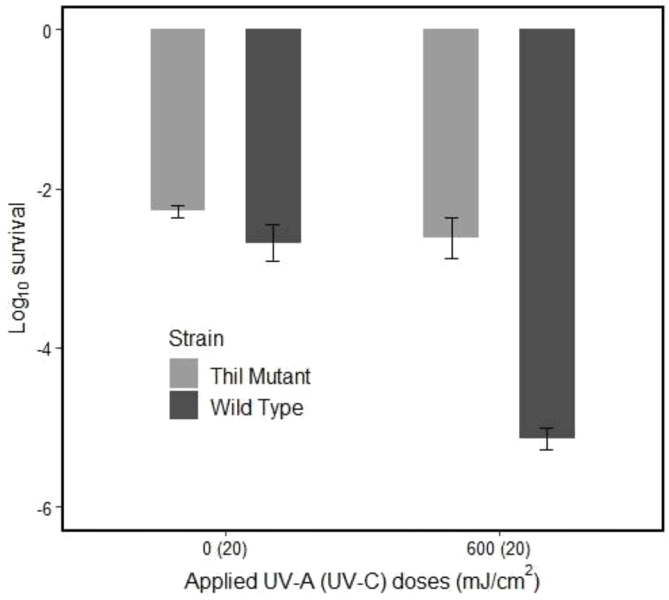

Fig. 5. The effect of combined UV-A and UV-C on $\log_{10}$ survival of *E. coli* MG1655 (wild type) and *E. coli* SP11 (ThiI mutant). The cells of the ThiI mutant strain experienced lower decline when exposed to a combination of UV-A and UV-C irradiation. Error bars represent the standard error of five independent experimental replicates.

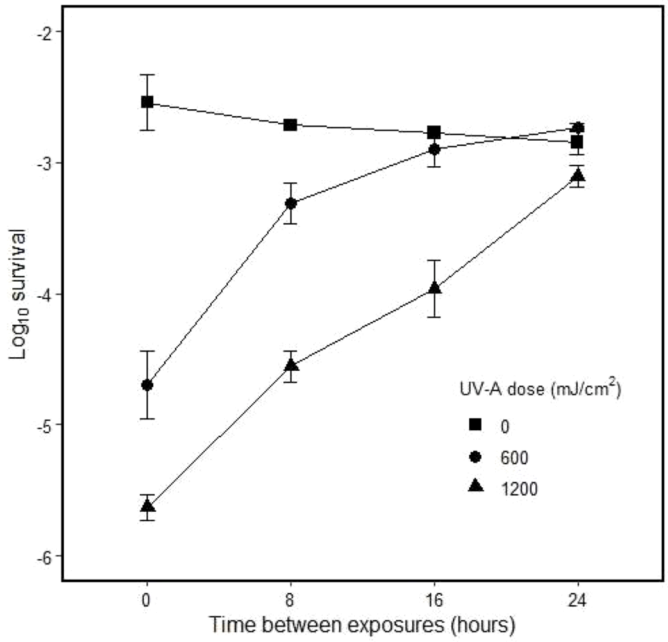

Fig. 6. Effect of the time delay between UV-A pre-exposure and 10 mJ/cm^2 of UV-C exposure on $\log_{10}$ survival. The higher the UV-A dose applied, the more time was required for the cells to recover prior to exposure to UV-C. The error bars represent the standard error of five independent experimental replicates.

after light exposure. Conversely, when applying 10 mJ/cm^2 of UV-C irradiation, there were approximately 17 times more cells immediately after exposure than 24 h later. This implies that only approximately 80 % and 95 % of the initial cell population remained inactivated for at least 24 h when exposed to 7.5 mJ/cm^2, and 10 mJ/cm^2 of UV-C irradiation, respectively. For samples that were exposed to UV-A prior to UV-C irradiation, the recovery was hindered compared to samples not pre-exposed to UV-A, but the difference was not statistically significant after 24 h or immediately after light exposure ($p = 0.02$). In the case of samples irradiated with 10 mJ/cm^2 of UV-C light after pre-exposure to 600 mJ/cm^2 of UV-A irradiation, 99.99 ± 0.01 % (mean ± SE) of the initial cell population remained inactivated after 24 h. In other words, samples pre-exposed to UV-A irradiation remained damaged 24 h later.

The impaired recovery from UV-C inactivation after UV-A light exposure is an important finding as the recovery of potentially pathogenic microorganisms after UV-C disinfection can be a health threat (Pullerits et al., 2020). The first reported observation that *E. coli* can recover after UV-C irradiation was in the 1940s (Roberts and Aldous, 1949). It was later connected to DNA repair, namely to the nucleotide excision repair (Harm, 1980). Another important pathway of recovery after UV-C irradiation is the regrowth of disinfection survivors. This is

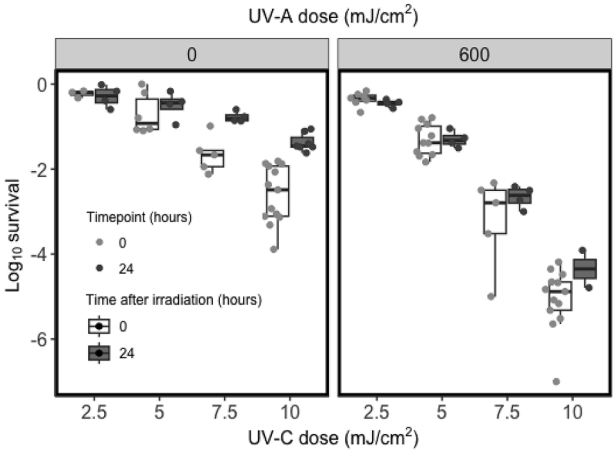

Fig. 7. Recovery of UV inactivated cells. Samples exposed to 600 mJ/cm^2 of UV-A light (right panel) and for the control without UV-A exposure (left panel) for different UV-C light intensities. The time of measuring the sample (0 or 24 h) had a significant influence on the photoinactivation.

especially important as they can grow on cell debris of cells killed in the UV-C inactivation, hence higher UV-C doses promote higher regrowth, which can be sustained for a longer time, as long as not every cell is dead (Kollu and Örmeci, 2015). It has been shown that regrowth is often the more important process in recovery of *E. coli* after UV-C disinfection than repair of UV damage (Bohrerova et al., 2015; Kollu and Örmeci, 2015).

4. Conclusion

Effective inactivation of bacteria in drinking water is very important for protecting public health. UV-C disinfection is a well-established technique that is expected to play an increasingly important role in drinking water disinfection. In this study, we investigated the potential of UV-A pre-exposure in enhancing UV-C disinfection of water, using *E. coli* as a model microorganism. Our findings revealed that applying UV-A irradiation prior to UV-C enhances the inactivation effect of *E. coli* with a synergistic effect. This synergistic effect relied on the presence of the s^{4}U modification in *E. coli* tRNAs. UV-A irradiated cells exhibited a growth delay which depended on the presence of thiolated uridine (s^{4}U) in the tRNA. The absorption of UV-A light by this chromophore induced a modified cellular state that facilitated a synergistic interaction with UV-C irradiation over an extended period. The magnitude of the synergistic effect was found to be dose-dependent when there was a time delay between the UV-A and the UV-C exposures. The synergistic effect was greatest when UV-A was applied immediately before UV-C; however, when there was a time lag between exposures (i.e. 16–24 h), the cells had more time to recover from the UV-A induced damage. Additionally, single cell experiments showed that once the cell growth resumed, the cell division time resembled that of unirradiated cells. Notably, a significant discovery of this study was the impaired recovery of UV-C treated cells following pre-exposure to UV-A irradiation; *E. coli* irradiated by UV-A prior to UV-C remained damaged 24 h later. Therefore, disinfecting water using UV-A followed by UV-C irradiation has the potential to enhance the effectiveness of UV-C disinfection through the synergistic action of both UV wavelengths while also impairing the recovery of UV-C treated cells. Future research involving real water samples and a comprehensive investigation into the behavior of a broad spectrum of bacteria is recommended for a robust validation and potential practical application of our results.

CRediT authorship contribution statement

Sandra Probst-Rüd: Conceptualization, Formal analysis, Investigation, Methodology, Project administration, Writing – original draft, Writing – review & editing. **Paul Onkundi Nyangaresi:** Data curation, Formal analysis, Writing – original draft, Writing – review & editing. **Adefolawe A. Adeyeye:** Data curation, Formal analysis, Writing – review & editing. **Martin Ackermann:** Conceptualization, Funding acquisition, Methodology, Project administration, Resources, Supervision, Writing – review & editing. **Sara E. Beck:** Data curation, Supervision, Funding acquisition, Resources, Writing – original draft, Writing – review & editing. **Kristopher McNeill:** Conceptualization, Funding acquisition, Methodology, Resources, Supervision, Writing – review & editing, Project administration.

Declaration of competing interest

The authors declare that they have no known competing financial interests or personal relationships that could have appeared to influence the work reported in this paper.

Data availability

Data will be made available on request.

Acknowledgments

This work was supported by the Swiss Federal Institute of Technology in Zurich (ETHZ) and the Swiss Federal Institute of Aquatic Science and Technology (Eawag). This research was partially supported by an Eawag Postdoctoral Fellowship for S. Beck as well as NSERC (Natural Sciences and Engineering Research Council of Canada) Discovery Grant RGPIN-2021–03560 through UBC. We thank Daan Kiviet for assistance with microfluidics, Tamar Kohn for her helpful comments on the analysis, Ryan Morin for assistance with Fig. 7, and Thusitha Rathnayake for creating the graphical abstract.

Supplementary materials

Supplementary material associated with this article can be found, in the online version, at doi:10.1016/j.watres.2024.121189.

References

Arnoldini, M., Vizcarra, I.A., Peña-Miller, R., Stocker, N., Diard, M., Vogel, V., Beardmore, R.E, Hardt, W.D., Ackermann, M., 2014. Bistable expression of virulence genes in salmonella leads to the formation of an antibiotic-tolerant subpopulation. PLoS Biol. 12 (8), e1001928 https://doi.org/10.1371/journal.pbio.1001928.

Beck, S.E., Hull, N.M., Poepping, C., Linden, K.G., 2018. Wavelength-dependent damage to adenoviral proteins across the germicidal UV spectrum. Environ. Sci. Technol. 52 (1), 223–229. https://doi.org/10.1021/acs.est.7b04602.

Beck, S.E., Ryu, H., Boczek, L.A., Cashdollar, J.L., Jeanis, K.M., Rosenblum, J.S., Lawal, O.R., Linden, K.G., 2017. Evaluating UV-C LED disinfection performance and investigating potential dual-wavelength synergy. Water Res. 109, 207–216. https://doi.org/10.1016/j.watres.2016.11.024.

Beck, S.E., Wright, H.B., Hargy, T.M., Larason, T.C., Linden, K.G., 2015. Action spectra for validation of pathogen disinfection in medium-pressure ultraviolet (UV) systems. Water Res. 70, 27–37. https://doi.org/10.1016/j.watres.2014.11.028.

Besaratinia, A., Yoon, J.I., Schroeder, C., Bradforth, S.E., Cockburn, M., Pfeifer, G.P., 2011. Wavelength dependence of ultraviolet radiation-induced DNA damage as determined by laser irradiation suggests that cyclobutane pyrimidine dimers are the principal DNA lesions produced by terrestrial sunlight. Faseb J. 25 (9), 3079–3091. https://doi.org/10.1096/fj.11-187336.

Bohrerova, Z., Rosenblum, J., Linden, K.G., 2015. Importance of recovery of *E. coli* in water following ultraviolet light disinfection. J. Environ. Eng. 141 (6), 04014094 https://doi.org/10.1061/(ASCE)EE.1943-7870.0000922.

Bommisetti, P., Bandarian, V., 2022. Site-specific profiling of 4-thiouridine across transfer RNA genes in *Escherichia coli*. ACS. Omega 7 (5), 4011–4025. https://doi.org/10.1021/acsomega.1c05071.

Bosshard, F.S., 2010. Mechanisms of Cell Damage in Enteric Bacteria During Solar Disinfection (SODIS). Swiss Federal Institute of Technology Zürich. Retrieved from.

https://www.research-collection.ethz.ch/bitstream/handle/20.500.11850/152016/eth-1417-02.pdf.
Cadet, J., Sage, E., Douki, T., 2005. Ultraviolet radiation-mediated damage to cellular DNA. Mutat. Res. 571 (1–2), 3–17. https://doi.org/10.1016/j.mrfmmm.2004.09.012.
Caldeira de Araujo, A., Favre, A., 1986. Near ultraviolet DNA damage induces the SOS responses in *Escherichia coli*. EMBO J. 5 (1), 175–179. https://doi.org/10.1002/j.1460-2075.1986.tb04193.x.
Čavužić, M., Liu, Y., 2017. Biosynthesis of sulfur-containing tRNA modifications: a comparison of bacterial, archaeal, and eukaryotic pathways. Biomolecules 7 (1), 27. https://doi.org/10.3390/biom7010027.
Dai, Y., You, L., Chilkoti, A., 2023. Engineering synthetic biomolecular condensates. Nat. Rev. Bioeng. https://doi.org/10.1038/s44222-023-00052-6.
Dullin, D., Mill, T., 1982. Development and evaluation of sunlight actinometers. Environ. Sci. Technol. 16, 815–820. https://doi.org/10.1021/es00105a017.
Favre, A., Chams, V., Caldeira de Araujo, A., 1986. Photosensitized UVA light induction of the SOS response in *Escherichia coli. Biochimie* 68(6), 857–864. 10.1016/S0300-9084(86)80101-8.
Hamamoto, A., Mori, M., Takahashi, A., Nakano, M., Wakikawa, N., Akutagawa, M., Ikehara, T., Nakaya, Y., Kinouchi, Y., 2007. New water disinfection system using UVA light-emitting diodes. J. Appl. Microbiol. 103 (6), 2291–2298. https://doi.org/10.1111/j.1365-2672.2007.03464.x.
Harm, W., 1980. Biological Effects of Ultraviolet Radiation. Cambridge University Press, New York.
Hoerter, J.D., Arnold, A.A., Kuczynska, D.A., Shibuya, A., Ward, C.S., Sauer, M.G., Gizachew, A., Hotchkiss, T.M., Fleming, T.J., Johnson, S., 2005. Effects of sublethal UVA irradiation on activity levels of oxidative defense enzymes and protein oxidation in *Escherichia coli*. J. Photochem. Photobiol. B Biol. 81 (3), 171–180. https://doi.org/10.1016/j.jphotobiol.2005.07.005.
Ishaq, M.S., Afsheen, Z., Khan, A., & Khan, A. (2018). Disinfection Methods. In K. Sher Bahadar & A. Kalsoon (Eds.), *Photocatalysts - Applications and attributes* (pp. Ch. 1). Rijeka: IntechOpen.
Itani, N., El Fadel, M., 2023. Microbial inactivation kinetics of UV LEDs and effect of operating conditions: A methodological critical analysis. Sci. Tot. Environ. 885, 163727.
Jagger, J., 1983. Physiological effects of near-ultraviolet radiation on bacteria. Photochem. Photobiol. Rev. 7, 1–75. https://doi.org/10.1007/978-1-4684-4505-3_1. Boston, MA: Springer US.
Jiang, Y., Rabbi, M., Kim, M., Ke, C., Lee, W., Clark, R.L., Mieczkowski, P.A., Marszalek, P.E., 2009. UVA generates pyrimidine dimers in DNA directly. Biophys. J. 96 (3), 1151–1158. https://doi.org/10.1016/j.bpj.2008.10.030.
Kneissl, M., Seong, T.Y., Han, J., Amano, H., 2019. The emergence and prospects of deep-ultraviolet light-emitting diode technologies. Nat. Photonics 13 (4), 233–244. https://doi.org/10.1038/s41566-019-0359-9.
Kollu, K., Örmeci, B., 2015. Regrowth potential of bacteria after UV in absence of light and dark repair. J. Environ. Eng. 141 (3), 04014069 https://doi.org/10.1061/(ASCE)EE.1943-7870.0000905.
Laszakovits, J.R., Berg, S.M., Anderson, B.G., O'Brien, J.E., Wammer, K.H., Sharpless, C. M., 2017. p-Nitroanisole/pyridine and p-nitroacetophenone/pyridine actinometers revisited: quantum yield in comparison to ferrioxalate. Environ. Sci. Technol. Lett. 4 (1), 11–14. https://doi.org/10.1021/acs.estlett.6b00422.
Martin-Somer, M., Pablos, C., Adan, C., van Grieken, R., Marugan, J., 2023. A review on led technology in water photodisinfection. Sci. Total Environ. 885, 163963.
Mathis, R., Ackermann, M., 2016. Response of single bacterial cells to stress gives rise to complex history dependence at the population level. Popul. Biol. 113 (15), 4224–4229. https://doi.org/10.1073/pnas.1511509113.
Meulemans, C.C.E., 1987. The basic principles of UV–disinfection of water. Ozone Sci. Eng. 9 (4), 299–313. https://doi.org/10.1080/01919518708552146.
Nyangaresi, P.O., Qin, Y., Chen, G., Zhang, B., Lu, Y., Shen, L., 2018. Effects of single and combined UV-LEDs on inactivation and subsequent reactivation of *E. coli* in water disinfection. Water Res. 147, 331–341. https://doi.org/10.1016/j.watres.2018.10.014.
Nyangaresi, P.O., Rathnayake, T., Beck, S.E., 2023. Evaluation of disinfection efficacy of single UV-C, and UV-A followed by UV-C LED irradiation on *Escherichia coli, B. spizizenii* and MS2 bacteriophage, in water. Sci. Total Environ. 859, 160256 https://doi.org/10.1016/j.scitotenv.2022.160256.
Probst-Rüd, S., McNeill, K., Ackermann, M., 2017. Thiouridine residues in tRNAs are responsible for a synergistic effect of UVA and UVB light in photoinactivation of *Escherichia coli*. Environ. Microbiol. 19 (2), 434–442. https://doi.org/10.1111/1462-2920.13319.
Pullerits, K., Ahlinder, J., Holmer, L., Salomonsson, E., Öhrman, C., Jacobsson, K., Dryselius, R., Forsman, M., Paul, C.J., Rådström, P., 2020. Impact of UV irradiation at full scale on bacterial communities in drinking water. NPJ. Clean. Water 3 (1), 11. https://doi.org/10.1038/s41545-020-0057-7.
Ramabhadran, T.V., Jagger, J., 1976. Mechanism of growth delay induced in *Escherichia coli* by near ultraviolet radiation. Proc. Natl. Acad. Sci. U.S.A 73 (1), 59–63. https://doi.org/10.1073/pnas.73.1.59.
Roberts, R.B., Aldous, E., 1949. Recovery from ultraviolet irradiation in *Escherichia coli*. J. Bacteriol. 57 (3), 363–375. https://doi.org/10.1128/jb.57.3.363-375.1949.
Song, K., Mohseni, M., Taghipour, F., 2019. Mechanisms investigation on bacterial inactivation through combinations of UV wavelengths. Water Res. 163, 114875 https://doi.org/10.1016/j.watres.2019.114875.
Sun, C., Limbach, P.A., Addepalli, B., 2020. Characterization of UVA-induced alterations to transfer RNA sequences. Biomolecules. 10 (11) https://doi.org/10.3390/biom10111527.
Thiam, K., Favre, A., 1984. Role of the stringent response in the expression and mechanism of near-ultraviolet induced growth delay. Eur. J. Biochem. 145 (1), 137–142. https://doi.org/10.1111/j.1432-1033.1984.tb08532.x.
Thomas, G., Favre, A., 1975. 4-thiouridine as the target for near-ultraviolet light induced growth delay in *Escherichia coli*. Biochem. Biophys. Res. Commun. 66 (4), 1454–1461. https://doi.org/10.1016/0006-291X(75)90522-7.
Wang, P., Robert, L., Pelletier, J., Dang, W.L., Taddei, F., Wright, A., Jun, S., 2010. Robust growth of *Escherichia coli*. Curr. Biol. 20 (12), 1099–1103. https://doi.org/10.1016/j.cub.2010.04.045.
World Health Organization (WHO)., 2022. Drinking water. Accessed on 30/03/2023. https://www.who.int/news-room/fact-sheets/detail/drinking-water.